



Optical Properties and Anti-Bacterial Activity of CdO:Zn Nanoparticles

R Santhi^{1,2*}, C Shanthi², M Sathya³ and K Pushpanathan³

¹Department of Physics, Mahendra Institute of Engineering and Technology, Namakkal - 637 503, India

²Department of Physics, Sona College of Technology, Salem - 636 005, India

³Nanomaterials Research Laboratory, Department of Physics, Government Arts College, Karur- 639 005 India

ABSTRACT

In this article we present a simple, efficient, low cost synthesis of CdO /CdZnO nanoparticles. The synthesized particles were characterized by x-ray diffraction, ultraviolet-visible spectroscopy, field emission scanning electron microscopy, photoluminescence spectroscopy and inductively coupled plasma measurements. X-ray diffraction studies indicate that the obtained CdO /CdZnO have a cubic structure at nanoscale. The band gaps were calculated from the absorption peak of ultraviolet-visible spectrum and it was found to vary from 2.47 - 2.28 eV on Zn doping. Increase in transmittance upon Zn doping was observed. Field emission scanning electron microscopy images showed that the synthesized samples composed of nanoparticles with the average diameter of 20.8 – 34.7 nm. The 6% Zn doped CdO nanoparticles were used to study antibacterial activities against Bacillus subtilis and Klebsiella pneumoniae microbes. It shows the antimicrobial activities are better against Bacillus subtilis than that of Klebsiella pneumoniae.

Keywords: CdO Nanoparticles; Antimicrobial activities; XRD; UV-Vis spectrum; FESEM

INTRODUCTION

In recent years, synthesis and characterization of binary chalcogenides of II–VI group semiconductor materials in nanometer scale has been a rapidly growing area of research, due to their exceptional chemical and physical properties that are different from those of either bulk material or single atom [1,2]. Nanomaterials of conducting oxides like cadmium oxide (CdO), zinc oxide (ZnO), tin dioxide (SnO₂), indium oxide (In₂O₃) and titanium oxide (TiO₂) have attracted the deliberation of researchers over the last two decades by reason of their outstanding applications in solar cells, flat panel displays, photovoltaic devices, smart windows and optical transmission devices. Of the above mentioned conducting oxides, CdO is the first reported transparent n-type semiconducting oxide (TCO). Eventhough it was first reported conducting oxide; it has not been widely studied as much of other oxide material like SnO₂, ZnO and In₂O₃, owing to its relatively small energy gap 2.2–2.7 eV with a direct band gap and 1.36–1.98 eV with indirect band gap [3]. This low band gap results the low optical conductivity in short wave length region. As a result, the physical properties of CdO could be improved for optoelectronic applications by doping with indium (In), tin(Sn), aluminium(Al), scandium, zinc (Zn) and yttrium (Y) which tunes its n-type conductivity and increases the band gap. Moreover, CdO nanoparticles are mainly used in photovoltaic cells, solar cells, phototransistors, IR reflectors, transparent electrodes, gas sensors and in variety of other materials. As it has high reflectance in the infrared region, together with high transparency (above 70%) in the visible region, it is also used as heat mirrors. Nanocrystalline CdO not only has unique optical and opto-electrical characteristics but it also has catalytic properties that make the compound suitable for use in the photodegradation of toxic organic compounds, dyes, pigments and other environmental pollutants [4]. In addition to optoelectronic applications, CdO nanoparticles have antibacterial effect. Investigation of antibacterial effect of CdO nanoparticles on Staphylococcus Aureus bacteria shows that the bacteria growth rate is declined by the CdO nanoparticles [5,6]. Antibacterial activities of different concentration of the CdO nanoparticles were tested on *E. coli* (Gram -ve) cultures Shukla et al.[7], and this study indicates that CdO nanoparticles show effective antibacterial activity toward the gram-negative bacterium *E. coli*. In similar fashion, the antimicrobial activities of CdO nanoparticles on *E.coli* cultures found that the CdO nanoparticles

show effective antimicrobial activity. Furthermore, it is reported that CdO nanowires have strong antimicrobial effect against *B.subtilis* (gram +ve) than that of *E.coli* (gram-ve) microbes [8].

A variety of nanostructures has been reported in CdO, which include nanoparticles [9], nano clusters [10], nanowires, nanorods [11], nanobelts [12], nanocubes [13], and rhombus-like Nanostructure [14]. All these nanostructures are being synthesized by several techniques. Ashoka et al. [15], and Barve et al. [16], followed a facile hydrothermal process with a post-reaction calcination to prepare the nanomaterials. Biological synthesis of CdO nanoparticles, using flower broth of *A. wilhelmsii* has been demonstrated by Karimi et al., [17]. Likewise Kalpanadevi et al., [18] succeeded in the preparation of CdO nanostructures from the low temperature thermal decomposition of inorganic precursors whereas sol-gel method has been proposed by de Anda Reyesa et al.,[19]. A well-known solvothermal method has been followed by Ghosh et al.,[20] have obtained the CdO nanoparticles by the decomposition of the cupferron complex in the presence of tri-n-octylphosphine oxide (TOPO). A simple and rapid microwave - assisted combustion method was developed to synthesize CdO nanospheres by Selvam et al., [21]. This valuable information motivated us to work in CdO nanostructures.

There are a number of articles discuss the synthesis of CdO nanoparticles, nanowires and nanofilms by chemical co-precipitation method [22,23]. Preparation of CdO nanoparticles using cadmium acetate and ammonia solution has been reported in Ref. no [24]. So, we have also chosen the chemical precipitation method here for the synthesis of CdO nanostructures, in view of the fact that an extensive literature review infers that chemical precipitation method is the principal method for the synthesis of metal oxide nanoparticles. Because it is a low temperature process, and easy to control the particle size and low cost method. In our previous work [25], we confirmed that precipitation method gives the smaller nanoparticle with good optical properties, in comparison with other synthesis procedure such as sol-gel synthesis, hydrothermal reaction and electrochemical routes. Hence, precipitation method has been adopted for the present work. For the above mentioned applications of CdO nanoparticles, we were interested in this work in the optical and antibacterial properties of CdO nanoparticles as a function of Zn composition.

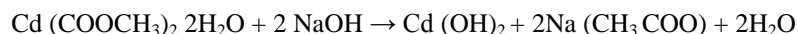
EXPERIMENTAL PROCEDURE

Materials and method

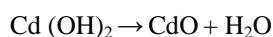
Analytical grade cadmium acetate dihydrate [$\text{Cd}(\text{COOCH}_3)_2 \cdot 2\text{H}_2\text{O}$], zinc acetate [$\text{Zn}(\text{CH}_3\text{COO})_2 \cdot 2\text{H}_2\text{O}$] sodium hydroxide (NaOH) and Polyethylene Glycol (PEG MW:400) supplied by Merck were used to synthesize undoped CdO and Zn doped CdO nanoparticles. All these chemicals were used without further refinement. The beaker and other glass wares used in this work were washed with acid. Ethanol and double distilled water were used as solvent for sample preparation. The detailed synthesis process was as follows

Synthesis of CdO and Zn doped CdO nanoparticles

CdO and different concentration of Zn doped CdO nanoparticles were efficiently synthesized by simple precipitation method using the above mentioned chemicals. Three samples were synthesized for the present study. The mechanism for the growth of CdO nanoparticles from cadmium acetate dihydrate precursor can be explained as follows. Initially, cadmium acetate dihydrate precursor is first dissolved in the mixture of water and ethanol and then hydrolyzed, which removes the intercalated acetate ions and results in cadmium hydroxide solution.



Then, during the calcination process at 400°C for 4 hrs, as prepared Cd (OH)₂ loses H₂O molecules then converted into CdO nanopowders. The overall reaction can be written as;



In a typical synthesis of CdO nanoparticle, 4 gm of cadmium acetate dihydrate and 2 gm of sodium hydroxide were dissolved in the mixture of water and ethanol in the ratio 1:1 under constant stirring of 400 rpm at room temperature (31°C) for 2 hrs. Cadmium acetate reacted with sodium hydroxide, and then converted into cadmium oxide. The cadmium oxide dispersion in distilled water and ethanol medium was clear and transparent and the solution was kept for 20 hrs in an air tight container in view of deposition of the powder. 2 ml of Polyethylene Glycol (PEG) was added as a capping agent. In this study, transparent solution of sodium acetate Na (CH₃COO) has been removed and the particles were washed several times using distilled water and ethanol, to remove the unreacted compounds. The powder thus obtained was dried at 120°C for 8 hrs to remove the remaining water content from the sample.

For the synthesis of Cd_{0.97}Zn_{0.03}O and Cd_{0.94}Zn_{0.06}O samples, appropriate amount of cadmium acetate and zinc acetate were dissolved in mixture of water and ethanol in the ratio 1:1 under the same experimental procedure.

However, 2 gm of NaOH were used for all the three samples. Then the samples were calcinated for 2 hrs at 400°C for 4 hrs which yielded nanoparticles with different sizes.

Characterization

The crystalline structure of the samples was analyzed by X-ray diffraction (XRD) using a Bruker AXSD8 Advance instrument equipped with Ni filtered CuK α radiation ($\lambda = 1.54187 \text{ \AA}$) in the range of 10-80° in steps of 0.0025 at a scan speed of 2°/min with scanning rate of 1°/min operated at 40 kV/30 mA. The morphology of the synthesized powder was examined by FE-SEM (JEOL – JSM – 6301 FE-SEM) operated at an accelerating voltage, above 5 kV/20 mA and a magnification of 5×10^4 . An inductively coupled plasma atomic emission spectrometer (ICP-AES; Varian Vista Pro, CCD Simultaneous, Springvale, Australia) was used for the determination of the Zn and Cd content of the nanopowders. To identify the functional groups and to confirm the presence Cd ions, the samples were examined with Fourier Transform Infrared Spectrometer Shimadzu-8400S spectrometer (Shimadzu Corporation, Kyoto, Japan) at a resolution of 2 cm^{-1} . The measurements were carried out in the region 400 – 4000 cm^{-1} using KBr as the beam splitter. Optical absorption and transmission spectra were recorded using Shimadzu-UV-2550-8030 (Shimadzu Corporation, Kyoto, Japan) UV– Vis spectrophotometer with a slit width of 5 nm and a light source change wavelength of 360 nm, at room temperature in the range of 190 to 800 nm. For this study, the nanopowders were dispersed in deionized water and mixed well. Finally, Photoluminescence (PL) response of the powder samples was carried out by means PL spectrometer (Kimon, SPEC-14031K, Japan) with a He-Cd laser source. A line spectrum of 350 nm has been used to excite the samples.

Anti-bacterial study

Analysis of antibacterial activities at different concentration is helpful in finding the optimum concentration that can have the most effective antibacterial property. Since, the antibacterial effect of undoped CdO nanoparticles on *E-coli* and has been already reported by many authors [26], here we investigated the effect of Cd_{0.94}Zn_{0.06}O nanoparticles on the growth of *Bacillus subtilis* (gram +ve) and *Klebsiella pneumonia* (gram -ve) by well diffusion method. In this method, the experiment is conducted in comparison with standard antibiotic solution by measuring the inhibition zone diameters.

In order to study the antibacterial activity, we mixed a known amount of calcinated Cd_{0.94}Zn_{0.06}O nanoparticles with distilled water in a glass beaker separately with the help of magnetic stirrer. As soon as the particles were dispersed in water the beaker was placed in an ultrasonicator for 40 minutes to go down the agglomeration. Then the so dispersed nanoparticles were prepared at five different concentration of 5 mg/ml, 10 mg/ml, 15 mg/ml, 20 mg/ml and 25 mg/ml. The Bacterial strains of *Klebsiella pneumoniae* and *Bacillus subtilis* were obtained from microbial type culture collection centre (MTCC), Chandigarh.

Agar well diffusion method

The antibacterial activity was studied using well diffusion method. 100 μl of aggressively growing target culture was affixed with 5ml of 1% top agar vortexed and pour onto the agar plate, allowed to solidify. The solidified plate was bored to form 7 wells of 6 mm diameter using cork borer. The wells were then inoculated with 100 μl aliquots of Cd_{0.94}Zn_{0.06}O nanoparticles from each concentration given above. They were allowed to diffuse into the agar followed by incubating the plates at 37°C for 48 hours. Upon incubation the zone of clearance around the wells were measured and evaluated.

RESULTS AND DISCUSSION

Structural characterization

The XRD patterns of CdO and Zn doped CdO nanoparticles are shown in Figure 1. The diffraction peaks with $2\theta = 33.2, 38.5, 55.4, 65.9, \text{ and } 70.4^\circ$ correspond to the crystal plans of (111), (200), (220), (311) and (222) of single phase CdO face- centered cubic phase, respectively. However, the diffraction peaks are slightly shifted to higher angles.

The high intensity peaks (111) and (200) have been used to estimate the average crystalline size of sample with the help of Scherer equation $D = 0.89\lambda / \beta \cos\theta$, where λ , is the wavelength of the CuK α radiation (0.154056 nm), and θ is the peak position and β is the Full Width at Half Maximum (FWHM). The average crystallite size found to be ~21 nm, ~31 nm, and ~35 nm for CdO, Cd_{0.97}Zn_{0.03}O and Cd_{0.94}Zn_{0.06}O samples. Also the sharpness of XRD peaks indicates that particles are in crystalline nature. Further, no indication of secondary phases such as CdO₂, Cd (OH)₂, and CdCO₃ are detected in the XRD pattern, indicating the formation of CdO crystalline phase. It can be seen that the crystal size increases from about 21 nm (CdO) to 33 nm for (Cd_{0.94}Zn_{0.06}O). This is directly related to the crystallization of nanoparticle

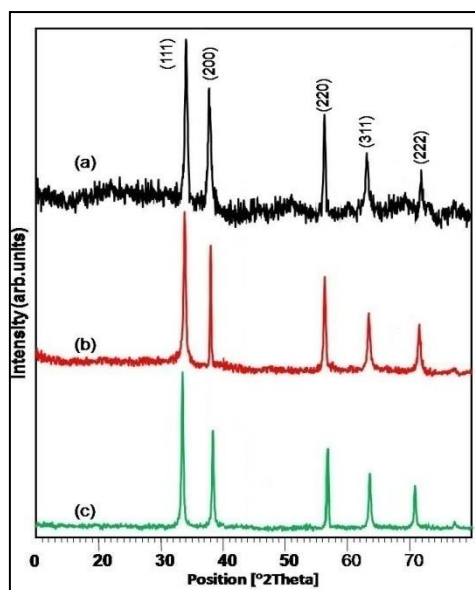


Figure 1: XRD patterns of the synthesized nanoparticles calcinated at 400°C where (a) CdO, (b) Cd_{0.97}Zn_{0.03}O, and (c) Cd_{0.94}Zn_{0.06}O nanoparticles

The lattice constant (a) and volume of the unit cell (V) calculated from the XRD data using the following equation. $a = \sqrt{3} d_{(111)}$, $V = a^3 \text{ nm}^3$, respectively. Since (111) peak has the highest intensity in the cases, this peak was considered for the lattice constant calculation also. Therefore, the lattice constant of CdO and Zn doped CdO was refined and found to be $a = \sim 4.676$ (2) Å, 4.679(5), and 4.6868(5) Å, respectively, which is lower than bulk CdO (4.695 Å) it matches well with the standard data for CdO nanoparticles reported in JCPDS Data Card No. (75–0594). Volume of the unit cell ($V = a^3$) is $\sim 103 \text{ Å}^3$. Further, the XRD profile shows that CdO nanoparticles are strongly crystallized with a preferred (111) orientation, which has been observed in previous work [27-29].

UV-Vis spectrum analysis

Figure 2 (a-c) shows the optical absorption versus wavelength of the CdO and Zn doped CdO nano powders. It is seen from these figures that the undoped CdO exhibits maximum absorption (λ_{max}) at 503 nm.

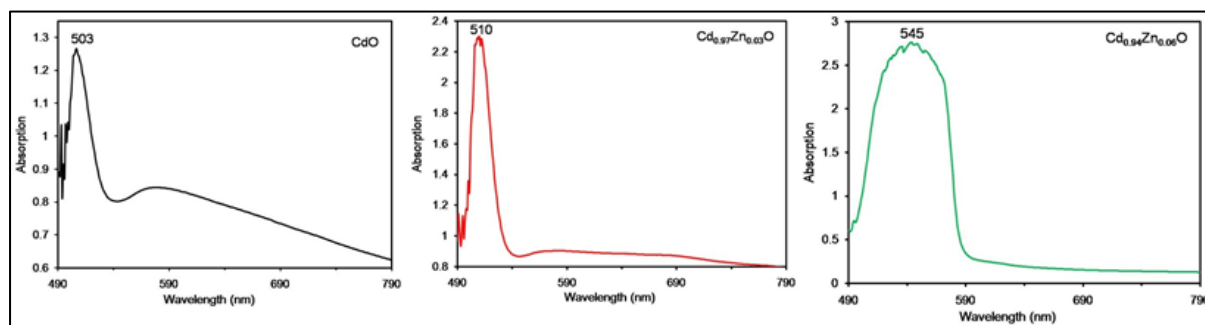


Figure 2: Optical absorption versus wavelength of the (a) CdO (b) Cd_{0.97}Zn_{0.03}O and (c) Cd_{0.94}Zn_{0.06}O nanopowders

A progressive red shift from 510 nm to 545 nm has been recorded as the Zn concentration increases from 3 (wt %) to 6 (wt %). This is attributed to the quantum size effect. The corresponding energy gap (E_g) for the reported three samples has been calculated using the equation

$$E_g = \frac{1240 \text{ eV}}{\lambda_{\text{max}}}$$

Where, h is Planck's constant ($6.626 \times 10^{-34} \text{ Js}$), c is the velocity of light, and λ_{max} is the excitonic absorption edge. The energy gap calculated to be 2.46, 2.43, and 2.28 eV for the samples of CdO, Cd_{0.97}Zn_{0.03}O and Cd_{0.94}Zn_{0.06}O samples, respectively. It can be seen that the band gap linearly decreases from 2.46 to 2.28 eV on doping. Helen and co-workers also found to decrease in energy gap of CdO with Zn doping [30]. Therefore,

UV-Vis spectrum analysis reveals that Zn doping decreases the energy gap of CdO nanoparticles. Table 1 shows the relation between Zn concentrations, lattice parameter, grain size; unit cell volume and energy gap of the synthesized samples and their pictorial representation is given in figure 3 (a,b).

Table 1: Lattice constant, unit cell volume undoped and Zn doped CdO nanoparticles

Sample	(hkl) value	Grain size 'D' (nm)	Average grain size	Interplaner distance (d) (Å)	Lattice constant 'a' (Å)	Unit cell volume 'V' (Å) ³
CdO	111	20.8	20.8	2.7121	4.697	103.62
	200	20.7		2.3476	4.695	103.49
Cd _{0.97} Zn _{0.03} O	111	29.9	30.5	2.7086	4.693	103.34
	200	31.2		2.3468	4.69	103.16
Cd _{0.94} Zn _{0.06} O	111	32.9	34.7	2.7134	4.698	103.69
	200	36.5		2.3471	4.693	103.34

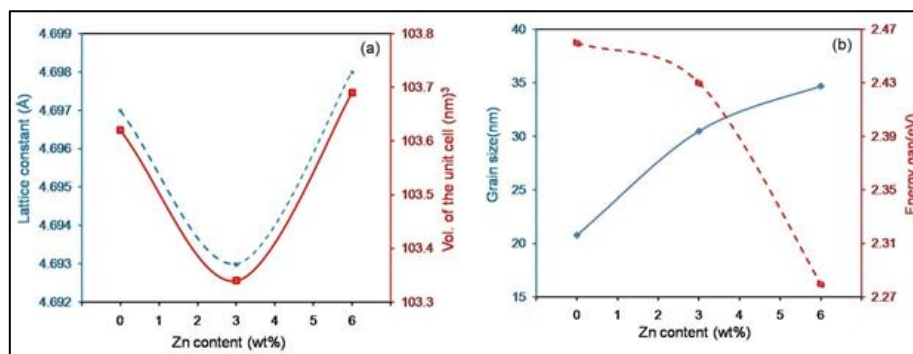


Figure 3: Graph displays the variation of (a) Zn content vs. lattice constant and unit cell volume, and (b) Zn concentration vs. grain size and energy gap of the CdO:Zn nanoparticles

The optical transmittance of the prepared nanopowders is displayed in figure 4. The undoped CdO shows the very low transmittance of 15% in the visible and near-IR region (530-1100 nm). It can be observed that the CdO nanoparticles doped with 3% of Zn shows the moderate transmittance of 30%. Furthermore, 6% Zn doping increased the transmittance maximum to 80%. This behaviour shows that Zn dopant enhances the optical transmittance of CdO. The transmittance graph presented here confirms that Zn doping in CdO matrix improves the transmittance by ~ 65 %. As limited articles are available on CdO:Zn nanoparticles, we unable to compare our result with others work.

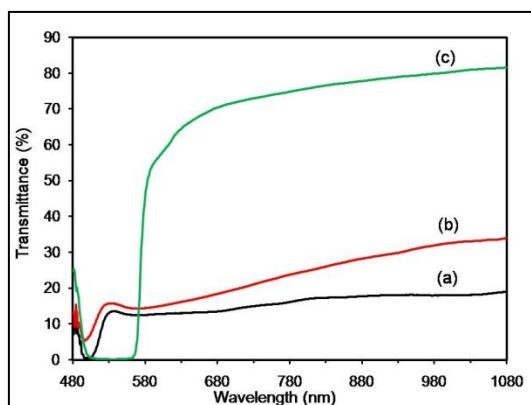


Figure 4: Transmittance spectrum of (a) CdO, (b) Cd_{0.97}Zn_{0.03}O, and (c) Cd_{0.94}Zn_{0.06}O nanoparticles shows that transmittance increases with Zn doping

Microstructure and composition analysis

The SEM micrographs of synthesized nanopowders of Cd_{1-x}Zn_xO (x = 0.00, 0.03, and 0.06) are shown in figure 5 (a-c). The undoped CdO sample has nanoparticles of spherical shape. It can be seen that some nanoparticles combined together and formed agglomeration. It should be noted that there is no voids. Particle size of undoped

CdO is estimated to be about 13 nm and uniformly distributed throughout the entire surface. (Figure 5a) The influence of Zn on CdO nanoparticles are clearly seen in the SEM images of the doped samples. Due to doping of 3(wt %) Zn, the morphology is changed from nanoparticle to rock like structure which is composed of nanoparticles and nano-rods. The interesting thing is that the addition of Zn ion cumulates many nanoparticles in a particular region there by creating the rock-like structure.

This accumulation of particles in a particular region creates voids between the grains. In some other regions, these small size nano-rods aligned themselves in the same direction which is highlighted in a box. Particle size also increased to 24 nm. This increase in particle size with Zn doping may be the fact of build up of some of doped Zn at crystallite boundaries which then enhances accumulation and fusion of crystallites forming larger grains and thus increases the particle size in comparison to the undoped CdO (Refer Figure 5b). In particular, we observed a dramatic change in microstructure from nanoplates to nano rods as the dopant concentration is further increased to 6 (wt %). This further increase in Zn ions results in increase in the size of the rock-like structure. Moreover, a large size nano-rod of nearly 800 nm length and 200 nm width can be seen in the 6(wt %) Zn doping (Figure 5c). We believed that this microstructural transformation could be attributed to the extremely small dimensions of the nanoparticles with high surface energy. Therefore, the SEM analysis infers that Zn ions cumulates the CdO nanoparticles and creates the nano rods. The rod-like CdO nanostructure is useful for gas sensing application, which is going on.

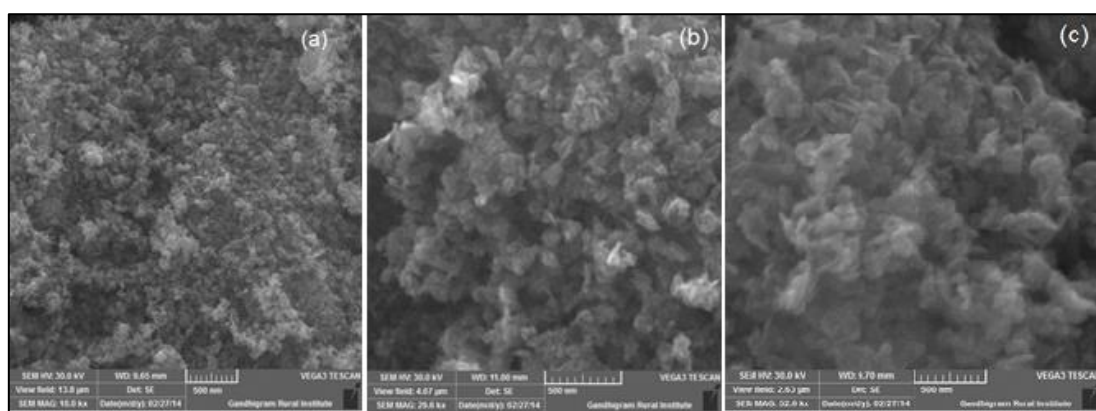


Figure 5: SEM image of the (a) CdO, (b) Cd_{0.97}Zn_{0.03}O, and (c) Cd_{0.94}Zn_{0.06}O nanoparticles

The analysis of the chemical composition by analytical quantitative technique like the ICP-AES is important because it establishes exactly how much Zn can be incorporated into CdO. It is already confirmed that for metal dopant ICP analysis more effective than energy-dispersive x-ray spectroscopy (EDS) analysis [31]. For that reason, composition of Zn doped CdO has been determined by ICP-AE analysis, which shows that the percentage of zinc in the prepared powder samples is nearly close to the concentration of Zn taken for synthesis (Table 2)

Table 2: Composition analysis of Zn doped CdO samples studied by ICP – AES

Composition used for sample preparation	ICP -AES		Composition based on ICP – AES analysis
	Cd (wt %)	Zn (wt %)	
Cd _{0.97} Zn _{0.03} O	96.2	2.8	Cd _{0.962} Zn _{0.028} O
Cd _{0.94} Zn _{0.06} O	93.4	5.6	Cd _{0.934} Zn _{0.056} O

Photoluminescence (PL) study

Figure 6 shows the PL spectra of the CdO and Zn doped CdO nanoparticles calcinated at 400°C recorded at room temperature. The PL spectrum displays three emission peaks. The less intensity peak appears at 431- 448 nm (2.87 – 2.77 eV) indicates the violet emission, 464 -484 nm (2.67 – 2.56 eV) indicates the blue emission and the peak between 504-516 nm (2.46 – 2.40 eV) corresponds the orange emission. The less intense violet emission peak is attributed to the transition from conduction band to the deep holes trapped levels i.e., Cadmium vacancies (V_{Cd}). The samples show two types of blue band they are blue band I (464 nm) and blue band II (484 nm). The blue band I is the result of cadmium intrinsic vacancy (Cd_i) and the intensity of this peak depends on the Cd_i . Blue band II at 484 nm can be ascribed to the direct recombination of conduction electron in the conduction band (Cd_{3d}) and a hole in the valance band (O_{2p}). Typical orange emission observed at 504-512 nm is from the positively charged single ion oxygen vacancy present on the surface of the nanoparticles. From PL study, it is clear that Zn doping favours for the violet emission in CdO nanoparticles. It has been reported that bulk CdO didn't show luminescence emission [24]. But we observed weak luminescence behaviour for undoped

CdO nanoparticle; it may be due to quantum size effect. As the Zn concentration increases, the intensity of violet emission increases and the peak shifted from 464 nm to 484 nm. It is the fact that the increasing Zn ion concentration decreases the number of defect sites which results in increase in intensity of the emission.

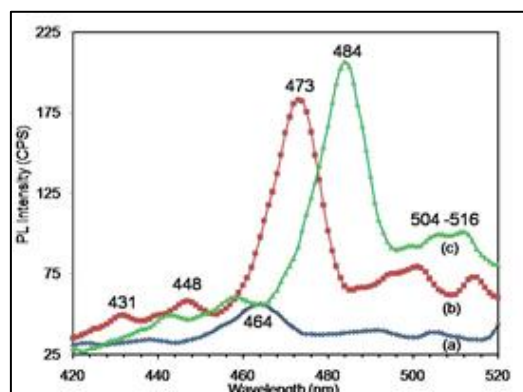


Figure 6: Room temperature PL spectrum of the synthesized nanoparticles (a) Undoped CdO, (b) Cd_{0.97}Zn_{0.03}O, (c) Cd_{0.94}Zn_{0.06}O nanoparticles. It shows that the peak shifted towards the longer wavelength as the Zn concentration increases

Fourier transform infrared spectroscopy study

Figure 7 depicts the FT-IR spectrum of the resulting nanopowders after heating treatment at 400 °C for 4h. The absorption bands that appeared evidently belong to the organic functional groups of the synthesized nanopowders. The absorption bands at 3605 cm⁻¹ and 3410 cm⁻¹ can be attributed to the asymmetrical and symmetrical stretching vibration bands of H₂O molecules, respectively. The observed vibration mode at 2923 cm⁻¹ and 1076 cm⁻¹ can be assigned to the C-H asymmetrical and symmetrical stretching vibrations, respectively. The peak centred at 2472 cm⁻¹ belongs to the absorption of CO₂ molecule from the air at the time of sample preparation. The specified weak peak at 1794 cm⁻¹ and broad peak at 1387 cm⁻¹ are assigned to C=O and C-O stretching vibrations of the carbonyl groups, respectively. Peaks below 1000 cm⁻¹ is useful in understanding the metal oxide bonding. In this sense, the strong narrow absorption bands at 719 cm⁻¹ represents the Cd-Zn-O bond exists in Zn doped samples and a weak peak at 485 cm⁻¹ represents the Cd-O phase [32]. It is interesting to note that incorporation of Zn atom decreased the broadness of the region between 1612 cm⁻¹ 1409 cm⁻¹, which implies that Zn concentration limits the vibration of carbonyl groups. Shift in the peak from 457 cm⁻¹ to 460 cm⁻¹ confirms the Zn dopant in the CdO nanocrystals. Likewise, Zn concentration also increased the intensity of absorption peak at 719 cm⁻¹. IT peak assignments are given in table 3. Therefore, the FTIR spectra confirmed the presence of Zn with the evidence of 858 cm⁻¹, 719 cm⁻¹ in the prepared samples.

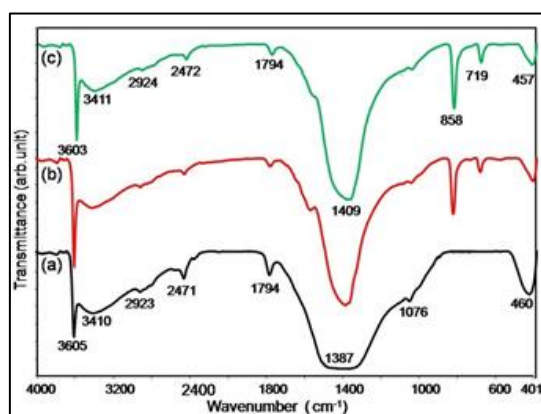


Figure 7: FTIR spectrum of the synthesized nanoparticles (a) undoped CdO, (b) Cd_{0.97}Zn_{0.03}O, (c) Cd_{0.94}Zn_{0.06}O nanoparticles

Assessment of antibacterial property

Result of agar diffusion test of Cd_{0.94}Zn_{0.06}O nanoparticles dispersed in distilled water against *Bacillus subtilis* and *Klebsiella pneumoniae* with inhibition zone around the cavity is shown in figures 8 and 9. It is observed that the area of the inhibition zone increases with the concentration in both bacteria.

Table 3: IR peaks and their assignments for prepared CdO:Zn nanoparticles

Assignments	Wavenumber (cm-1)		
	CdO	Cd _{0.97} Zn _{0.03} O	Cd _{0.94} Zn _{0.06} O
Asymmetrical stretching of H ₂ O molecules	3605	3604	3603
Symmetrical stretching of H ₂ O molecules	3410	3421	3411
C-H asymmetrical stretching vibrations	2923	2924	2924
C-H symmetrical stretching vibrations	1076	1075	1076
Absorption of CO ₂ molecule from the air	2471	2471	2472
C=O stretching vibrations	1794	1796	1794
C-O stretching vibrations	1387	1410	1409
Cd-Zn-O bond	-	858- 719	858- 719
Cd -O bond	460	448	457

Interestingly, in the present study Cd_{0.94}Zn_{0.06}O nanoparticles have shown high cell inhibition of 23 mm for *Bacillus subtilis* which is nearly equal to the inhibition zone of 23 mm to the standard antibiotics (Ciprofloxacin S^{*}). The zone of inhibition is found to be more for gram positive bacteria than gram negative bacteria. Assay of antibacterial activity of CdO: Zn Nanoparticles at different concentration is displayed in table 4.

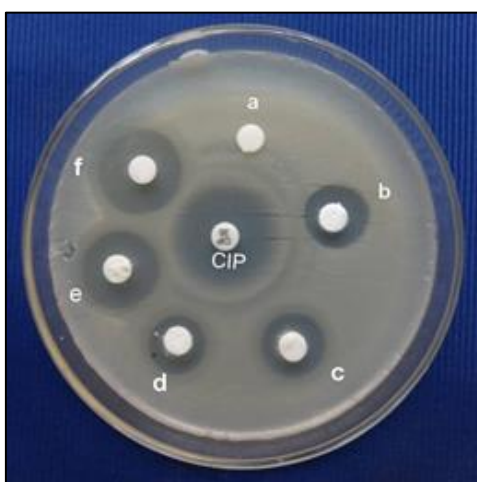


Figure 8: Image of antimicrobial activity of Cd_{0.94}Zn_{0.06}O nanopowders on *Bacillus subtilis* (gram -ve) at various concentration of (a) control (b) 5 mg/ml, (c) 10 mg/ml, (d) 15 mg/ml, (e) 20 mg/ml and (f) 25 mg/ml

It is reported that the undoped CdO microplates have strong antimicrobial effect against gram negative bacteria than gram positive bacteria. CdO nanoparticles have strong and almost equal antimicrobial effect of CdO nanoparticles against both gram negative bacteria (*E.coli*) and gram positive bacteria (*Bacillus subtilis*). Conversely, Kumar [8] observed that CdO nanowires have strong antimicrobial effect against *Bacillus subtilis* (gram +ve) than that of *E.coli* (gram-ve) microbes. These earlier reports clearly relay that antibacterial effect of CdO needs to be clarified further. But our study confirms that Zn ions present in the Cd_{0.94}Zn_{0.06}O nanoparticles damages the structure of *Bacillus subtilis* bacterial cell membrane and controls the activity of some membranous enzymes which kills the *Bacillus subtilis* bacteria ultimately. Therefore, our study demonstrates that Zn doped CdO nanoparticles can be useful in the treatment of infectious diseases caused by *Bacillus subtilis*.

Several researchers have suggested different possible mechanism involving in the interaction of nanomaterials with the microorganisms. Zhang and Chen [33] reported that every microorganism possess a positive charge. This positive charge creates an electromagnetic attraction between the microorganism and treated surface. The moment, the contact is made, the microbe is oxidized and die instantaneously. Likewise, Wang et al. suggested that in the aqueous system, both nanoparticles and bacteria tended to aggregate, and the nanoparticle toxicities were mainly attributed to the ions dissolved in the solutions [34]. In general, it is believed that when the nanomaterials are exposed to light, it produces so called reactive oxygen species (ROS) on the surface of these nanoparticles which react with the thiol groups (-SH) of the proteins present on the bacterial cell surface. Such proteins stick out through the bacterial cell membrane, allowing the transport of nutrients through the cell wall. Nano materials inactivate the proteins, decreasing the membrane permeability and eventually causing the cellular death.



Figure 9: Image of antimicrobial activity of $\text{Cd}_{0.94}\text{Zn}_{0.06}\text{O}$ nanopowders on *Klebsiella pneumoniae* (gram -ve) at various concentration of (a) control (b) 5 mg/ml, (c) 10 mg/ml, (d) 15 mg/ml, (e) 20 mg/ml and (f) 25 mg/ml

Table 4: Assay of antibacterial activity of CdO: Zn Nanoparticles at different concentration CIP* Ciprofloxacin (30 mg)

Bacteria	Zone of Inhibition (mm in diameter)						
	CIP*	(a) Control	(b) 5 mg/ml	(c) 10 mg/ml	(d) 15 mg/ml	(e) 20 mg/ml	(f) 25 mg/ml
<i>Bacillus subtilis</i> (gram +ve)	24	-	20	18	17	20	23
<i>K. pneumoniae</i> (gram +ve)	22	-	8	11	13	14	16

CONCLUSION

In conclusion, we have successfully synthesized the CdO and Zn doped CdO nanocrystals were synthesized by simple chemical precipitation method. XRD analysis confirms that the samples contain the nanosize particles. The energy gap calculation from UV-Vis analysis confirms that the prepared nanoparticles possesses indirect band gap and also it infers that Zn doping increases the band gap of CdO. The FESEM images of CdO clearly revealed that it has sphere-like structure of uniform nanoparticles with an average size of 29 nm. The morphology of the Zn doped CdO powder nano-rod and rock-like structure with the average size of 35 nm. We conclude that Zn doping align the CdO these nanoparticles in a particular direction and form the rock-like and nano-rod like morphology. Compositional analysis and FTIR analysis confirmed the presence of Zn in CdO matrix. PL analysis confirms that the Zn incorporation shift the emission of CdO from blue band I to blue band II. The anti-bacterial activities are better against *Bacillus subtilis* (gram +ve) than that of *Klebsiella pneumoniae* (gram-ve). Therefore, finally it is concluded that our study demonstrates that $\text{Cd}_{0.94}\text{Zn}_{0.04}\text{O}$ nanoparticles can be useful in the treatment of infectious diseases caused by *Bacillus subtilis*.

ACKNOWLEDGEMENT

Authors (CS and RS) are thankful to the Research Scholars M Jay Chithra, C Thangamani, M Ponnar and M Priyadharshni of Nanomaterials Research Laboratory, Department of Physics, Government Arts College, Karur for their timely help in the synthesis process.

REFERENCES

- [1] AN Ejhieh; Z Banan, *Desalination.*, **2011**, 279, 146-151.
- [2] N Rajkumar; VM Susila; K Ramachandran, *J. Exp. Nanosci.*, **2011**, 6, 389-398.
- [3] PH Jefferson; SA Hatfield; TD Veal; PDC King; CF Mc Connville; JZ Perez; VM Sanjose, *Appl. Phys. Lett.*, **2008**, 92, 022101.
- [4] A Tadjarodi; M Imani; H Kerdari; K Bijanzad; D Khaledi; M Rad, *Nanomaterials and Nanotechnology.*, **2014**, 4, 1-10.
- [5] T Ahmad; S Khatoun; K Coolahan; SE Lofland, *J. Mater. Res.*, **2013**, 28, 1245-1253.
- [6] B Salehi; S Mehrabian; M Ahmadi, *J. Nanobiotechnology.*, **2014**, 12:26.
- [7] M Shukla; S Kumari; S Shukla; RK Shukla, *J. Mater. Environ. Sci.*, **2012**, 3 (4) 678-685.
- [8] S Kumar; AK Ojha, *AIP Advances.*, **2013**, 3, 052109 - 052109.

- [9] DM Yufanyi; JF Tendo; AM Ondoh; JK Mbadcam, *J. Mater. Sci. Res.*, **2014**, 3, 1-14.
- [10] R Srinivasaraghavan; R Chandiramouli; BG Jeyaprakash; S Seshadr, *Spectrochimica Acta Part A, Molecular and Biomolecular Spectroscopy.*, **2013**, 102, 242–249.
- [11] W Li; M Li; S Xie; T Zhai; M Yu; C Liang; X Ouyang; X Lu; H Li; Y Tong , *Cryst.Eng.Comm.*, **2013**, 15 ,4212-4216.
- [12] ZW Pan; ZR Dai; ZL Wang, *Science.*, **2001**, 9, 1947-1949.
- [13] JH Kim; YC Hong; HS Uhm, *Jpn. J. Appl. Phys.*, **2007**, 46, 7A.
- [14] A Tadjarodi; M Imani, *Mater. Lett.*, **2011**, 65, 1025–1027.
- [15] S Ashoka; P Chithaiah; GT Chandrappa, *Mater. Lett.*, **2010**, 64, 173–176,
- [16] AK Barve; S M Gadegone; MR Lanjewar; RB Lanjewar, *Int J Recent Innov Trends Comput Commun*, **2014**, 2 ,2806 – 2810.
- [17] J Karimi Andeani; S Mohsenzadeh, *J. Chem.*, **2013**, 2013, Article ID 147613, 4 pages.
- [18] K Kalpanadevi; CR Sinduja; R Manimekalai, *ISRN Inorg Chem.*, **2013**, Article ID 823040, 5 pages.
- [19] DA Reyesa; GT Delgado; RC Perez; JM Marín; OZ Angelb, *J. Photochemistry and Photobiology A, Chemistry*, **2012**, 228, 22– 27.
- [20] M Ghosh ; CNR Rao, *Chem. Phys. Lett.*, **2004**, 393, 493–497.
- [21] NCS Selvam; RT Kumar; K Yogeenth; LJ Kennedy; G Sekaran; JJ Vijaya, *Powder Tech.*, **2011**, 211, 250–255.
- [22] RB Waghulade; PP Patil; R Pasricha, *Talanta*, **2007**, 72, 594-599.
- [23] AK Barve; SM Gadegone; MR Lanjewar; RB Lanjewar, *Int Conference Indust Autom Comput* **2014**, 35-38.
- [24] DD Vijaykarthik; M Kirithika; N Prithivikumaran; N Jeyakumaran, *Int. J.Nano. Dimens.* **2014**, 5, 557-562.
- [25] K Pushpanathan, S Sathya, M Jaychithra, S Gowthami, R Santhi, *Mater. Manuf. Process.*, **2012**, 27, 1334–1342.
- [26] K Karthik; S Dhanuskodi; C Gopinath; S Sivaramakrishnan, *J Innov Res Sci Engineer*, <http://ijirse.in/docs/ican14/ican105.pdf>
- [27] A Tadjarodi; M Imani; H Kerdari; K Bijanzad; D Khaledi; M Rad, *Nanomater. Nanotech.* **2014**, 4,16. DOI: 10.5772/58464.
- [28] C Sravani; KT Ramakrishna Reddy; P Jayarama Reddy, *Mater. Lett.* **1993**, 15, 356-358.
- [29] CH Bhosale; AV Kambale; KY Kokate, *Mater.Sci. Eng. B.* **2005**, 122, 67-71.
- [30] SJ Helen; D Suganthi; T Mahalingam, *Nat Conference Adv Technol Oriented M*, **2014**.
- [31] K Pushpanathan; K Vallalperuman; S Seenithurai; R Kodipandyan; M Mahendran, *Mod Phys Lett B*, **2011**, 25, 1577–1589.
- [32] L Hutt, A book on review of near infrared reflectance properties of metal oxide nanostructures, **2013**, GNS Science, ISBN: 9781972192849.
- [33] H Zhang; G Chen, *Environ. Sci. Technol.*, **2009**, 43, 2905-2910.
- [34] Z Wang; YH Lee; B Wu; A Horst; Y Kang; YJ Tang; DR Chen, *Chemosphere*, **2010**, 80, 525-529.